J. Crop Prot. 2016, 5 (4): 591-602
doi: 10.18869/modares.jcp.5.4.591

Research Article

Classification using radial-basis neural networks based on thermographic assessment of *Botrytis cinerea* infected cut rose flowers treated with methyl jasmonate

Mehrnoosh Jafari[1], Saeid Minaei[1*], Naser Safaie[2], Farah Torkamani-Azar[3] and Mehdi Sadeghi[4]

1. Department of Bio-System Mechanic Engineering, Faculty of Agriculture, Tarbiat Modares University, Tehran, Iran.
2. Department of Plant Pathology, Faculty of Agriculture, Tarbiat Modares University, Tehran, Iran.
3. Department of Electrical Engineering, College of Electrical and Computer Engineering, Shahid Beheshti University, Tehran, Iran.
4. Department of Horticultural Sciences, Faculty of Agriculture, Tarbiat Modares University, Tehran, Iran.

Abstract: Many environmental and physiological factors affect plant temperature. The objective of this study was to use thermal imagery to investigate robust features for early diagnosis of *Botrytis cinerea* infection in cut rose flowers under the postharvest application of Methyl Jasmonate (MeJA). Three cases treated with different concentrations of MeJA (0.1, 0.2, and 0.3 $\mu l.l^{-1}$), a control (0 $\mu l.l^{-1}$ MeJA) and an ethanol-treated case (20 $\mu l.l^{-1}$ ethanol) were considered as five treatments in this study. Infrared images of MeJA-treated and non-treated flowers were captured during five consecutive days. Eight days after inoculation, disease severity in all concentrations of MeJA was significantly lower than that of control and ethanol treatments. Maximum temperature difference (MTD) index and median temperature could be used to diagnose the existence and growth of fungal pathogen, at least a day before any significant visual symptoms appear. To identify some robust features for classifying the infected and non-infected flowers, analysis of temperature frequency distribution was implemented. Laplace and normal distributions were considered as the best fitted probability distributions based on the shape of thermal histograms. Parameters of normal and Laplace probability density functions were estimated and the most effective attributes were selected. A radial-basis-function neural network with 60 neurons in the hidden layer was designed to classify and distinguish the infected flowers from the healthy ones. Results showed that the network can classify the infected and non-infected flowers with a 96.4% correct estimation rate.

Keywords: Laplace distribution, Median temperature, Normal distribution, Thermal histogram

Introduction

Recent developments in technology and electronics have made it possible to visualize small temperature differences by the use of new highly sensitive thermal cameras. Plant temperature is a short term phenomenon affected by the incoming radiation, water status of the plant, and the environmental conditions such as air temperature, relative humidity and wind speed (Jones, 1992). Stomatal activities regulate the thermal reaction of a plant with its environment (Bajons *et al.,* 2005). As leaf temperature is negatively correlated to transpiration rate (Inoue *et al.*, 1990) and

Handling Editor: Masoud Shams-Bakhsh

* **Corresponding author**, e-mail: minaee@modares.ac.ir
Received: 29 November 2015, Accepted: 20 February 2016
Published online: 29 December 2016

[Downloaded from jcp.modares.ac.ir on 2024-10-12]

[DOR: 20.1001.1.22519041.2016.5.4.12.7]

directly related to the rate of evapotranspiration (Jones *et al.,* 2002), infrared sensing of the canopy temperatures can be used to monitor crop water stress, pre-symptom reaction to diseases, and plant physiological changes.

Detecting plant infection always occurs when visible symptoms appear or pathogens have been identified (Wang *et al.,* 2012). This time is often too late to stop the disease damage. Water status, respiration rate, cuticular and stomatal conductance of plant leaves may be affected by the disease which leads to significant modifications of plant temperature (Chaerle *et al.*, 1999). Potential for the use of thermal imagery to detect the pre-symptomatic appearance of plant disease has been investigated by some researchers. Resistance to tobacco mosaic virus (Chaerle, 1999), spatial and temporal changes in the transpiration rate of cucumber leaves infected with downy mildew (Lindenthal *et al.,* 2005, Oerke *et al.,* 2006), early diagnosis of bacterial wilt disease of tomato plants (Chiwaki *et al.,* 2005), localized decreases in temperature of apple leaves infected by scab disease (Oerke *et al.,* 2011), and the leaf response in cucumber plants infected with the soil-borne pathogen *Fusarium oxysporum* (Wang *et al.,* 2012) have been monitored by digital infrared thermography.

In most of the previous studies maximum temperature difference (MTD), defined as the difference between the highest and the lowest temperature within an area of interest, was used as a comparison index. The need for a reference temperature and the incorporation of environmental factors on MTD has been reported. Therefore, using the temperature frequency distribution and the analysis of differences over small distances to further improve the thermal analysis has been suggested (Stoll *et al.,* 2008).

Roses are important cut flowers which have more than 130 species and belong to Rosaceae family. Cut rose flowers are affected by many physiological changes from the harvest time to the time they reach the hands of consumers. These changes are the result of pre and post-harvest factors that lower the quality of flowers and their marketability (Serek *et al.,* 2006; Bhattacharjee and Banerji, 2010).

Botrytis cinerea Pers. is a ubiquitous fungal pathogen that causes gray mold in many fruits, vegetable and ornamental crops. This disease is a major problem for greenhouse flower producers worldwide. Synthetic chemical fungicides such as benzimidazoles and dicarboximides have long been relied on to reduce gray mold disease development. However, continuous use of these fungicides is problematic due to development of fungal resistance and increasing social and environmental concerns over chemical residues (Macnish *et al.*, 2010).

Several alternative strategies for reducing gray mold infection in rose flowers have been tested including exposure to elevated CO_2 atmospheres, inoculation with antagonistic microbes, treatment with calcium sulfate and use of growth regulators such as gibberellic acid, salicylic acid and Methyl Jasmonate (MeJA) (Macnish *et al.,* 2010). Methyl Jasmonate as plant signaling molecules can modulate flowering and senescence in higher plants. In addition, Jasmonates (Jasmonic acid and its ester) have been revealed to be involved in direct protection against biotic stresses. These compounds are considered to have a hub role in the intracellular signaling cascades which activate inducible plant defense systems (Meir *et al.*, 1998).

This study aims to test (1) whether thermal imagery can be used to sense and quantify the severity of gray mold disease in cut rose flowers under application of different concentrations of Methyl Jasmonate and (2) a radial-basis-function neural network is designed to classify infected versus non-infected flowers based on the extracted features of thermal histograms.

Materials and Methods

Plant materials

Rosa hybrid cv. 'Dolce vita' flowers were harvested from a commercial greenhouse (Abyek, Qazvin, Iran) based on commercial index in the early morning. Flowers were

[Downloaded from jcp.modares.ac.ir on 2024-10-12]

[DOR: 20.1001.1.22519041.2016.5.4.12.7]

immediately transferred to the Postharvest Physiology laboratory (Tarbiat Modares University, Tehran, Iran). Upon arrival to the laboratory, stems of cut flowers were placed in water for an hour for rehydration, and then stems were recut to 40 cm length. Then, flowers were placed in preservative solution containing 200 mgL^{-1} 8-hydroxyquinoline sulfate and 3% sucrose.

Methyl Jasmonate treatment

In order to apply Methyl Jasmonate vapor, cut rose flowers were placed in 200 liter glass chambers for 24 hours. The desirable volume of MeJA was mixed with 20 $\mu l.l^{-1}$ of ethanol and poured onto filter paper inside the glass chambers to meet the required concentrations of 0.0 (did not receive MeJA nor Ethanol), 0.1, 0.2 and 0.3 $\mu l.l^{-1}$MeJA, and then the glass chambers were immediately sealed. In addition, cut flowers were treated with only 20 $\mu l.l^{-1}$ of ethanol as control. After treatment of MeJA (24h), MeJA-treated and non-treated flowers were aerated for an hour and thereafter were inoculated with the spores of *Botrytis cinerea* for 12h. Six cut rose flowers were assigned to each treatment

Inoculation by fungal spores of *B. cinerea*

A culture of *B. cinerea* was obtained from naturally infected rose petals cv. 'Dolce vita' flowers and grown on potato dextrose agar (PDA). *B. cinerea* cultures were grown under 12h dark/12h NUV light at 20 ± 2 °C. Spore suspensions were prepared from the sporulating edges of 2-week-old *B. cinerea* cultures in petri plates. Spores were gently removed with a bacteriological loop, suspended in sterile distilled water (DW) and filtered through four layers of sterile cheese cloth to remove remaining mycelia. The spore concentration was determined with a haemocytometer and adjusted to 10^4 spores ml^{-1}. Prepared suspension was applied to the flowers by misting using a hand pump. After artificial inoculation, to maintain high relative humidity for establishing infection, once again flower containers were placed in glass chambers for 12h. Thereafter, flowers were removed from glass chambers and placed on benches at 20 ± 2 ºC, 65 ± 5% RH and a 12/12h light/dark photoperiod at an illumination of 15 $\mu molm^{-2}s^{-1}$.

Thermal image acquisition

Digital thermal images were obtained using a non-cooled focal-plane-array infrared camera (ITI-P400, ITI Infrared AB., Sweden). The instrument operates in the waveband of 8–14 µm. The detector array has a geometric resolution of 25 µm (384 × 288 pixels focal plane array and a 21.7° × 16.4° field of view lens with a minimum focus distance of 0.3 m). The thermal resolution is 0.08 °C and the accuracy of absolute temperature measurement is less than ± 2 °C. Throughout the entire experiment the emissivity was fixed at 0.95. The imager was mounted on a tripod and positioned 30 cm above the flowers. ITI-P400 is also equipped with a CMOS sensor, 2 Mega pixels resolution visible camera. Therefore, the original visible images with Jpeg format, RGB color space and the 482 × 642 pixels image size, were captured. Next, images were analyzed using ITI-IrAnalyser (ITI Infrared AB., Sweden) software. Using this software, images were saved in Jpeg format, grayscale palette, and temperature range of 15 to 30 ºC.

For five days, from the day of inoculation (denoted as 0 dpi (days post inoculation)) to four days after inoculation, images were taken (Fig. 1). Before commencing the measurements, the camera was acclimatized to laboratory conditions for at least 30 min. Measurements were conducted once a day between 15:00 pm to 17:00 pm.

Image processing procedure

Image processing was conducted using Matlab R2010 software. To facilitate the image processing operation, a black surface was used as the background of all visible pictures. Flowers were initially detected using only their R-component of visible image and a binary image was obtained (Fig. 2 (a) & (b)). This is necessary to note that to remove spurious white pixels and to smoothen the white contours from the binary image, therefore, a morphological

[Downloaded from jcp.modares.ac.ir on 2024-10-12]

[DOR: 20.1001.1.22519041.2016.5.4.12.7]

opening operation (erosion followed by dilation) was applied.

ITI-P400 cameras capture zoomed thermal images; therefore, the captured thermal pictures were resized to the suitable size (232 × 310 pixels). Subsequently, the Canny edge detection was chosen to determine the edges of the flower. Since, in Canny edge detection algorithm, Gaussian kernel convolution was used before edge detection, only the strong edges of the thermal image were detected. To eliminate noise and distinguish the relative strong edges, a range and a scale, and consequently a threshold was determined based on the maximum and minimum convolution values. The normalized cross-correlation of the edge-detected thermal and original visible images was computed and coordinates of peak were determined, accordingly. Finally, the total offset between the images was identified and consequently, thermal and original visible images were registered (Fig. 2 (c)).

Thermal histograms assessment

Thermal histograms were developed and parameters of probability distributions that best fitted the thermal data were estimated. Based on the shape of the thermal histograms, it was assumed that the standard normal and the Laplace distributions could be selected (Fig. 3).

Both the normal and Laplace distributions are described by two parameters. Equations 1 and 2 show the probability density functions of normal and Laplace distributions, respectively.

Normal distribution:

$$P(x) = \frac{1}{b\sqrt{2\pi}} e^{-\frac{(x-a)^2}{2b^2}} \quad (1)$$

Laplace distribution:

$$P(x) = \frac{1}{2b} e^{-\frac{|x-a|}{b}} \quad (2)$$

Here, a is a location parameter such as the mean of the probability while b, which is sometimes referred to as the diversity, is a scale parameter ($b \geq 0$). A normal and a Laplace distribution for $a = 0$ and $b = 1$ are shown in Fig. 4.

'*fit*' function of *Matlab* software was used to determine a and b parameters for the best fitting of histogram data to the normal and Laplace distributions. Also, this function gives the parameters of R^2, and standard error of estimate (SSE) for each fitting as the important fitted performances. Other information such as skewness and goodness of fitting may be demonstrated using Q-Q plots.

A Q-Q Plot is a plot of the percentiles (or quintiles) of a distribution against the corresponding percentiles of the observed data. If the observations follow approximately the specified distribution, the resulting plot should be roughly a straight line with a positive slope.

Therefore, to design a classifier; thermal histograms and thermal features such as temperature maximum and minimum, median, MTD, R^2 of fitting data to the standard normal and Laplace distribution curve, as well as parameters of the normal and Laplace probability density functions were computed.

Radial-basis neural network classifier

When a Radial-Basis-Function (RBF) network is used to perform a complex pattern classification task, the problem is basically solved by transforming it into a high-dimensional space in a nonlinear manner. Based on Cover's theorem, a complex pattern-classification problem cast in high-dimensional space nonlinearly is more likely to be linearly separable than in a low-dimensional space (Haykin, 1999).

Radial-Basis-Function networks consist of three fixed layers (Fig. 5). The first layer is composed of input nodes whose number is equal to the dimension of input vector. The second layer is a hidden layer, composed of units with radial-basis-activation functions (RBF) that are connected directly to all of the nodes in the input layer. The output layer consists of a linear summation unit. As Gaussian activation functions are often used in the hidden layer, therefore the corresponding layer is called *Gaussian (kernel) layer* (Haykin, 1999).

Attribute selection

Flowers were ranked based on daily inspection: '-1' was assigned to the healthy and '1' was designated for the diseased samples. Eleven

[Downloaded from jcp.modares.ac.ir on 2024-10-12]

[DOR: 20.1001.1.22519041.2016.5.4.12.7]

different features were evaluated to select the most effective features for correct classification of the infected and non-infected flowers. These included: maximum temperature, minimum temperature, MTD, median temperature, a_n and b_n parameters of the standard normal probability function, a_l and b_l parameters of the standard Laplace probability function, R_n^2 of fitting thermal data to the standard normal distribution, R_l^2 of fitting thermal data to the standard Laplace distribution and skewness. To find a good subset, the features were plotted against classes and the predictive ability of each feature was evaluated by considering the correlation with classes.

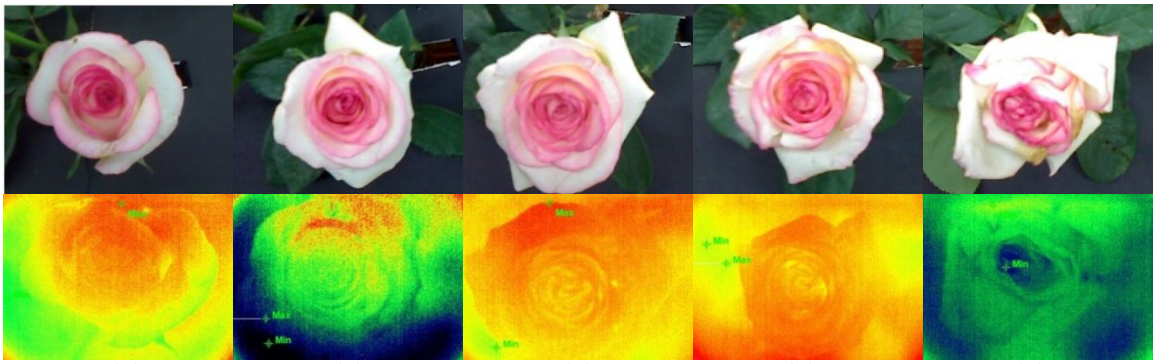

Figure 1 Top row: Captured original pictures of a control flower in different days; bottom row: thermal images corresponding to the top original pictures, dpi: days post inoculation.

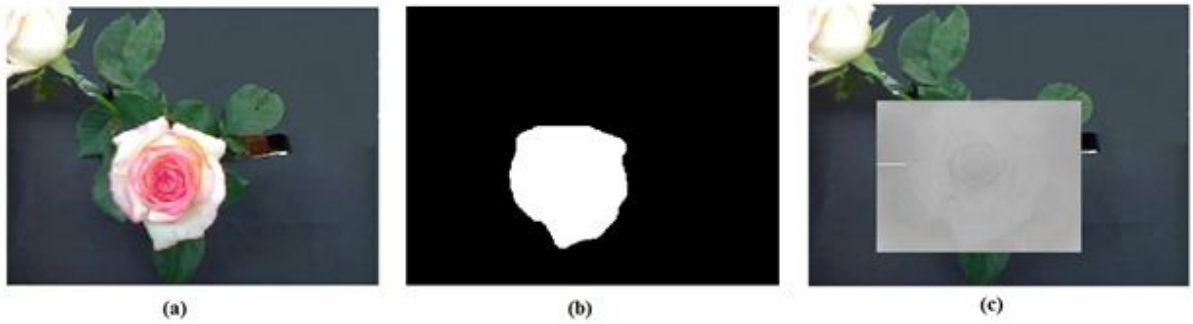

Figure 2 Image segmentation procedure, a) visible image, b) flower detected image, c) registered thermal image using visible image.

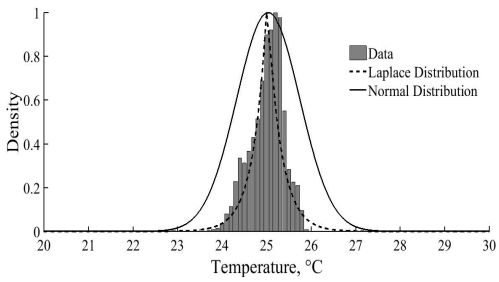

Figure 3 Thermal histogram of an Ethanol-treated flower one day post inoculation, along with the fitted standard normal and standard Laplace distributions.

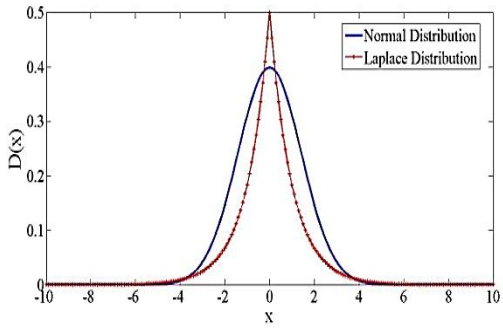

Figure 4 Normal and Laplace probability density plots with the location and scale parameters of zero and unity, respectively.

[Downloaded from jcp.modares.ac.ir on 2024-10-12]

[DOR: 20.1001.1.22519041.2016.5.4.12.7]

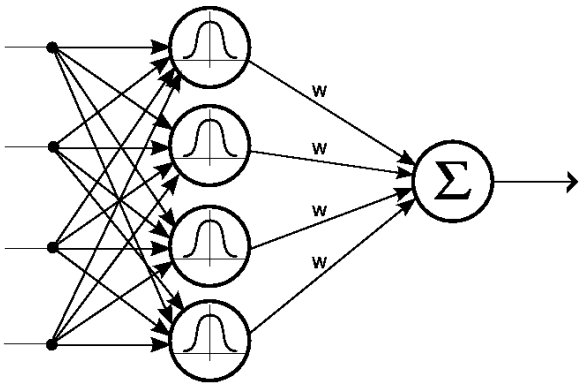

Figure 5 Three layers of a radial-basis-function neural networks.

RBF network design

Selected attributes formed the input matrix and a target class vector was made based on the ranked flowers. Mean square error goal and spread were set to 0 and 0.1, respectively. After training the network, the following parameters were determined:

1- Number of neurons in the hidden layer.
2- Coordinates of the center of each hidden-layer RBF function.
3- Radius (spread) of each RBF function in each dimension.
4- The weights applied to the RBF function outputs as they are passed to the output layer.
5- Network output

A Radial-Basis-Function Neural Network was designed to test the predictive ability of some combinations of features. The data set contained 140 samples, in which 110 random samples were used for training and 30 random samples were used for testing the network. Correct class estimation performance was calculated based on the following commands in Matlab Software:

correct = 100 × (length(find(T. × O > 0))/length (T)

T: Target class vector
O: Network output vector
correct: Percent of correct estimation

Based on the network response, three subsets yielded the best classification results (Table 1). However, the network demonstrated its best classification rate with an input matrix containing a_n and b_n-estimated parameters of the normal probability density function. However, training and testing the network with an input matrix containing a_l and b_l-estimated parameters of the Laplace probability density function was also admissible (Table 1).

Disease assessments

To assess the disease severity, a completely randomized design with three replications was considered. Disease assessments were carried out in MeJA-treated and non-treated flowers from 12 hours to 8 days after artificial inoculation. Disease severity was evaluated daily based on the following arbitrary scale: 0, no lesions on the petals; 1, 1–5% petal surface area (SA) affected by lesions; 2, 5–25% SA affected by lesions; 3, 25–50% SA affected by lesions; and 4, 50-100% SA affected by lesions (Darras, 2005).

Results and Discussion

Results of daily visual inspection

MeJA treatments significantly reduced disease incidence in cut rose flowers inoculated with *B. cinerea*. Daily observations indicated that 4, 5, 6, 7 and 8 days after inoculation, the symptoms of gray mold in MeJA-treated flowers were significantly lower than those in ethanol treatment or control (Fig. 6). Analysis of variance indicated that treatments, vase life, and their interaction were statistically significant ($P < 0.01$) (Table 2). In ethanol and control treatments, flowers did not show any signs of disease until the second day; while in the concentrations of 0.1, 0.2 and 0.3 $\mu l.l^{-1}$ MeJA, they did not show any symptoms until the third day. Disease severity in all concentrations of MeJA eight days post inoculation (dpi) was significantly lower than that in controls (73.1%) and ethanol (66.3%).

[Downloaded from jcp.modares.ac.ir on 2024-10-12]

[DOR: 20.1001.1.22519041.2016.5.4.12.7]

Table 1 Attribute selection based on the Radial-Basis-Neural-Network response.

Number of neurons in the hidden layer	Correct estimation (%)					
	Max. & Median Temperature		a_n & b_n		a_l & b_l	
	Train	Test	Train	Test	Train	Test
20	79.09	50	87.27	76.67	85.45	73.33
40	86.36	63.33	91.82	80.00	89.09	73.33
60	92.73	80	96.36	86.67	93.64	76.67
80	96.36	76.67	97.27	83.33	99.09	80.00

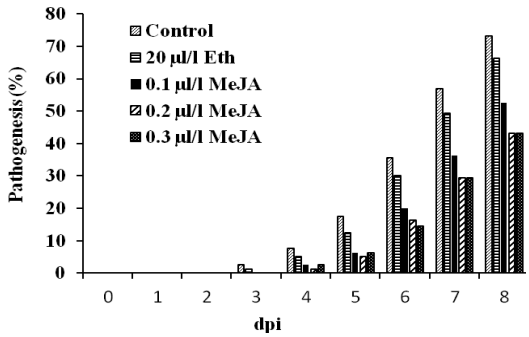

Figure 6 Results of disease incidence in cut rose flowers inoculated with *B. cinerea* ranked based on arbitrary scale, Eth: Ethanol, MeJA, Methyl Jasmonate, dpi: days post inoculation.

Table 2 Analysis of variance of the effects of MeJA on *Botrytis cinerea* pathogenesis in cut rose flowers.

Source	df	Mean square
Between Treatments		
Treatments	4	1150.674**
Error	10	60.541
Within Time		
Time	8	7532.880**
Time × Treatment	32	186.470**
Error (Time)	80	13.599
CV (%)	-	22.93

ns, not significant; *, $P < 0.05$; **, $P < 0.01$.

Thermal assessment

In 0 dpi, a significant difference in median temperature was seen between the treatments. The treatment which received 0.3 µl.l^{-1}MeJA had the highest median temperature, and consequently, the median temperature decreased in accordance with the decrease in concentrations of MeJA (0.3 > 0.2 > 0.1 > control > 0 µl.l^{-1}MeJA) (Fig. 7).

Since all the flowers were brought out of glass chambers before image acquisition one day post inoculation (1 dpi), no significant difference was observed between the median temperatures of treatments (Fig. 7).

Control and ethanol treatments had the highest median temperature after the first day (2 dpi, 3 dpi, 4 dpi). This difference was plausible considering the severity of gray mold (Fig. 7).

One day post inoculation, thermal images clearly indicated that an increase of temperature up to 1 °C occurs at infected points. Histopathology interaction of *Botrytis cinerea* and rose flowers has shown that infection of healthy petals starts with penetration of the cuticle by the conidial germ tubes via open stomata (Pie and De Leeuw, 1991). At this stage of pathogen growth, transpiration of infected areas decreases due to stomatal closure. After penetration, pegs enlarged to form infection hyphae, which invaded the periclinal wall of outer epidermal cells. Subsequently, intra- and intercellular growth of hyphae led to a collapse of epidermal and mesophyll cells and the lesions became necrotic. Eventually, the necrosis would spread leading to death of the whole petal (Pie and De Leeuw, 1991). Thermal assessment showed that the lesions had a lower temperature than the surrounding healthy petals, it might be a result of uncontrolled loss of water from damaged cells.

In addition, with regard to MTD index, results showed that control and ethanol treatments, reached the highest numerical value of MTD index one day post inoculation (1 dpi), and it decreased during the following days (Fig. 8).

[Downloaded from jcp.modares.ac.ir on 2024-10-12]

[DOR: 20.1001.1.22519041.2016.5.4.12.7]

However, MeJA-treated flowers demonstrated their maximum MTD two days post inoculation.

If MTD index is considered as an indicator of fungal pathogen growth, usage of 0.1, 0.2 and 0.3 $\mu l.l^{-1}$ MeJA is seen to postpone the fungal activity for at least 24 hours. However, the numerical value of MTD index was not related to the disease severity since the presence of necrosis resulted in a lower MTD. Altogether, before any significant visual symptoms appeared on the infected flowers, commencement of fungal activity was detectable using MTD index. Previous research work indicated that MTD and plant temperature can be affected by the environmental factors (Stoll *et al*., 2008). To identify the robust features that would be useful in classifying flowers, analysis of the thermal histograms was undertaken.

Q-Q plots

Q-Q plot of the thermal data vs. the standard normal distribution is shown in Fig. 9a. As can be seen, thermal data exhibits deviation from the straight line. At most points, numerical values of normal distribution are much higher than the thermal histogram. In addition, Q-Q plot of the thermal data vs. the standard Laplace distribution is given in Fig. 9b. Comparison of the thermal histograms of all the treatments and repetitions indicated healthy plants exhibit a thermal histogram similar to the standard Laplace distribution. Infection with fungal pathogen caused the thermal histograms to deviate from Laplace distribution and shift to the normal one.

Classification with Radial-Basis-Function Neural Networks

Network response was evaluated by changing the maximum number of the hidden layer neurons (Fig. 10). Results showed that the network can classify the flowers at a 96.4% correct estimation rate by using 60 neurons in the hidden layer (Table 3). In spite of the fact that 100% correct estimation would be achievable by increasing the number of neurons in the hidden layer, however, the network's output would have to pass through all the data points which would decrease the accuracy of classification for the new datasets. Hence, sixty would be the best figure for the number of neurons in the hidden layer (Fig. 10).

It is necessary to note that the discussed CPU times are those computed by Matlab software. In real time implementation, all hidden layer nodes could operate in parallel which leads to much shorter CPU times.

A large number of neurons in the hidden layer was expectable, because in this research only the temperature was measured and also there were different disease severities. Extracting more robust features by using visible image processing, NIR spectroscopy, or multispectral images is recommended.

Conclusion

Daily inspection showed that disease severity in all concentrations of MeJA eight days after inoculation was significantly lower than those in controls and ethanol treated samples. Median temperature and MTD index were capable of diagnosing the existence and growth of fungal pathogen, at least one day before any visible symptoms were detectable on the flowers. Results showed that analysis of temperature frequency distribution and considering the shape of the thermal histogram would be more effective in classifying healthy and diseased plants than the comparison indices such as MTD and median temperature.

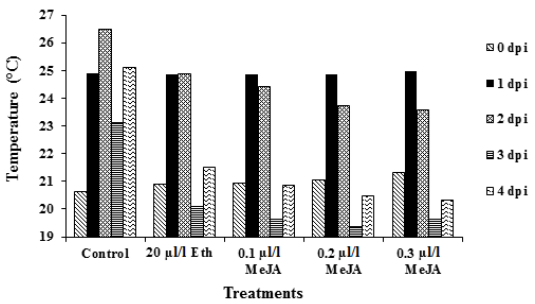

Figure 7 Median temperature of treatments in five consecutive imaging days, Eth: Ethanol, MeJA: Methyl Jasmonate, dpi: days post inoculation.

[Downloaded from jcp.modares.ac.ir on 2024-10-12]

[DOR: 20.1001.1.22519041.2016.5.4.12.7]

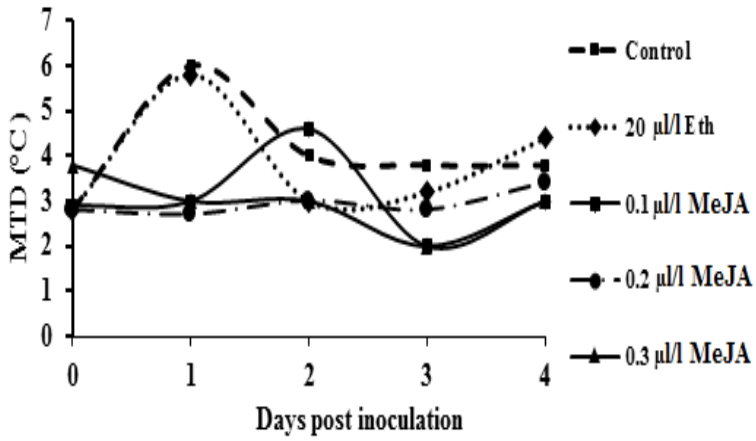

Figure 8 Variation in MTD index for each treatment during five consecutive imaging days, Eth: Ethanol, MeJA: Methyl Jasmonate, dpi: days post inoculation.

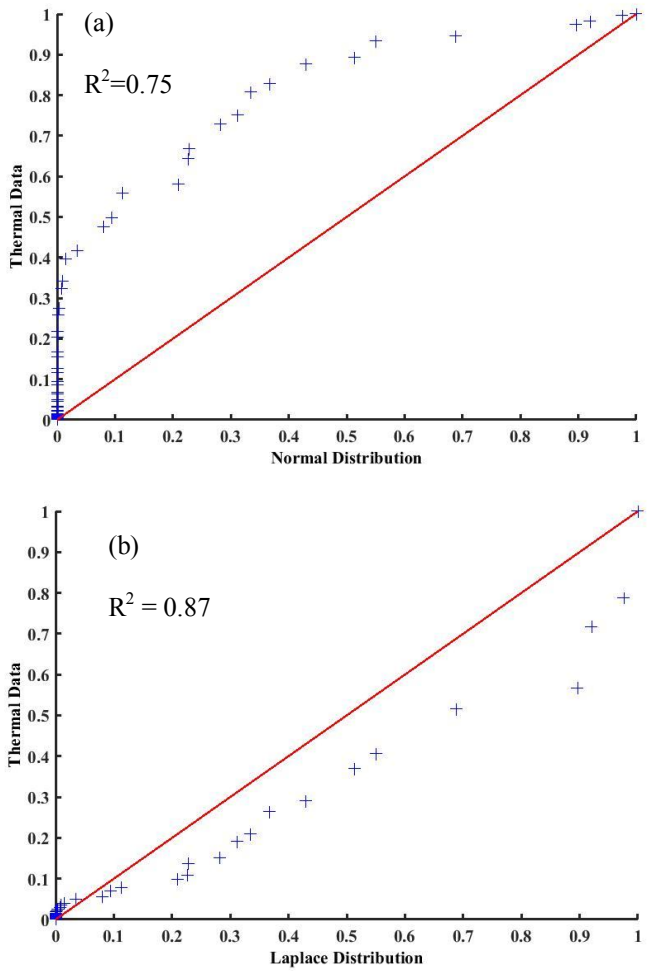

Figure 9 Q-Q plot of an Ethanol-treated flower one day post inoculation, against: a) standard normal and b) standard Laplace distribution.

[Downloaded from jcp.modares.ac.ir on 2024-10-12]

[DOR: 20.1001.1.22519041.2016.5.4.12.7]

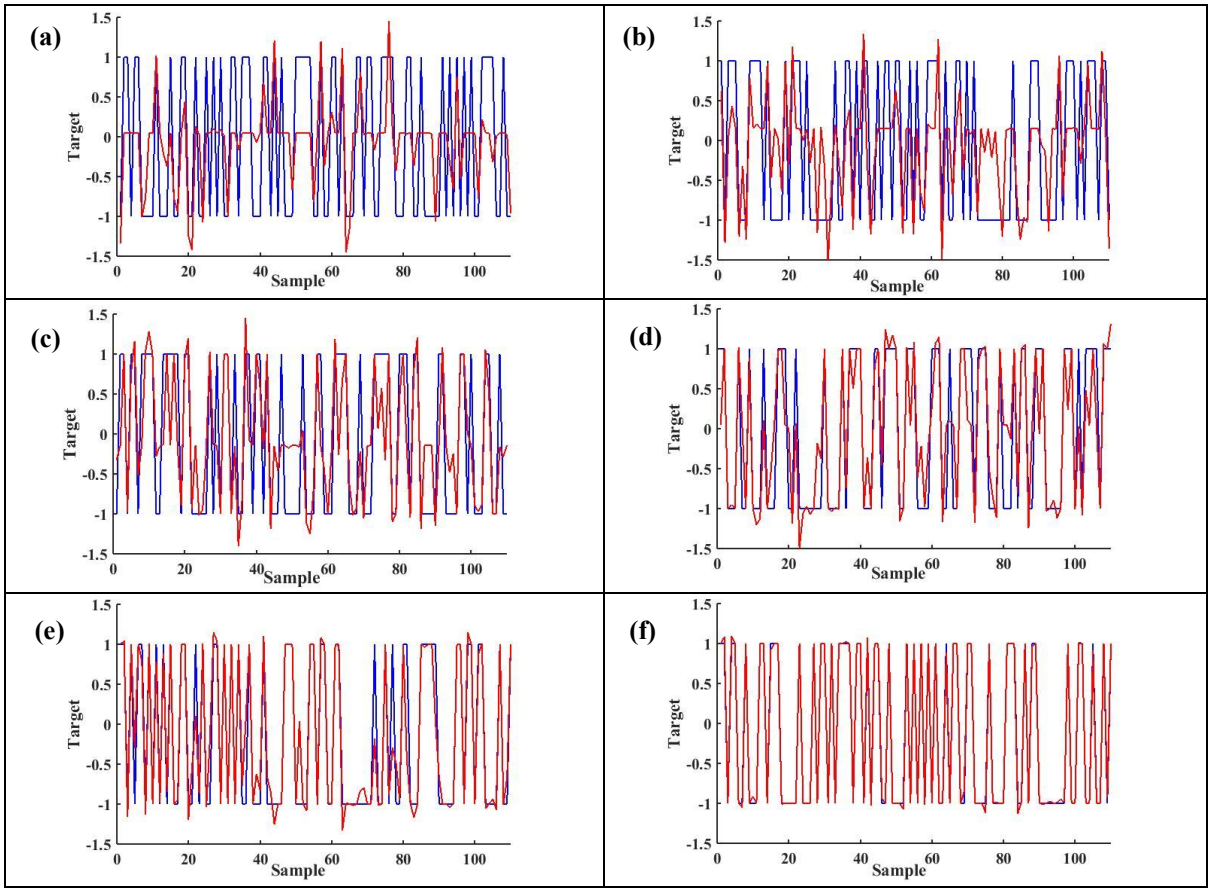

Figure 10 RBF classifier response as affected by the number of neurons in the hidden layer, a) 10, b) 20, c) 40, d) 60, e) 80 and f) 100 neurons, ——, Target; ——, Network Output.

Table 3 Network response as affected by the number of neurons in the hidden layer.

Number of neurons in the hidden layer	MSE	Correct estimation (%)		CPU Time (sec)
		Train	Test	
10	0.56	80.00	73.33	1.11
20	0.44	87.27	76.67	1.31
40	0.27	91.82	80.00	2.34
60	0.14	96.36	86.67	3.22
80	0.10	97.27	83.33	4.24
100	0.01	100	70	5.14

References

Bajons, P., Klinger, G. and Schlosser, V. 2005. Determination of stomatal conductance by means of infrared thermography. Infrared Physics and Technology, 46: 429-439.

Bhattacharjee, S. K. and Banerji, B. K. 2010. The Complete Book of Roses, Aavishkar Publisher, India.

Chaerle, L., Van Caeneghem, W., Messens, E., Lambers, H., van Montagu, M. and van der Straeten, D. 1999. Presymptomatic visualization of plant–virus interactions by thermography. Nature Biotechnology, 17: 813-816.

Chiwaki, K., Nagamori, S. and Inoue, Y. 2005. Predicting bacterial wilt disease of tomato plants using remotely sensed thermal

[Downloaded from jcp.modares.ac.ir on 2024-10-12]

[DOR: 20.1001.1.22519041.2016.5.4.12.7]

imagery. Journal of Agricultural Meteorology, 61 (3): 153-165.

Darras, A. I., Terry, L. A. and Joyce, D. C. 2005. Methyl jasmonate vapour treatment suppresses specking caused by *Botrytis cinerea* on cut Freesia hybrid L. flowers. Postharvest Biology and Technology, 38: 175-182.

Haykin, S. 1999. *Neural Networks*: *A Comprehensive Foundation*, 2nd Edition, Prentice-Hall.

Inoue, Y. 1990. Remote detection of physiological depression in crop plants with infrared thermal imagery. Japanese Journal of Crop Science, 59: 762-768.

Jones, H. G. 1992. Plant and microclimate, 2nd Edition, Cambridge University Press, Cambridge, UK.

Jones, H. G., Stoll, M., Santoa, T., De Sousa, C., Chaves, M. M. and Grant, O. M. 2002. Use of infrared thermography for monitoring stomatal closure in the field: application to grapevine. Journal of Experimental Botany, 53: 2249-2260.

Lindenthal, M., Steiner, U., Dehne, H. W. and Oerke, E. C. 2005. Effect of Downy mildew development on transpiration of cucumber leaves visualized by digital infrared thermography. Phytopathology, 95 (3): 233-240.

Oerke, E. C., Steiner, U., Dehne, H. W. and Lindenthal, M. 2006. Thermal imaging of cucumber leaves affected by downy mildew and environmental conditions. Journal of Experimental Botany, 57: 2121-2132.

Oerke, E. C., Fröhling, P. and Steiner, U. 2011. Thermographic assessment of scab disease on apple leaves. Precision Agriculture, 12 (5): 699-715.

Pie, K. and De Leeuw, G. T. N. 1991. Histopathology of the initial stages of the interaction between rose flowers and *Botrytis cinerea*. Netherlands Journal of Plant Pathology, 97: 335-344.

Stoll, M., Schultz, H. R., Baecker, G. and Berkelmann-Loehnertz, B. 2008. Early pathogen detection under different water status and the assessment of spray application in vineyards through the use of thermal imagery. Precision Agriculture, 9: 407-417.

Serek, M., Woltering, E., Sisler, E., Frello, S. and Sriskandarajah, S. 2006. Controlling ethylene responses in flowers at the receptor level. Biotechnology Advances. 24: 368-381.

Macnish, A. J., Morris, K. L., De Theije, A., Mensink, M. G. J., Boerrigter, H. A. M., Reid, M. S., Jiang, C. Z. and Woltering, E. J. 2010. Sodium hypochlorite: A promising agent for reducing *Botrytis cinerea* infection on rose flowers. Postharvest Biology and Technology, 58: 262-267.

Meir, Sh., Droby, S., Davidson, H., Alsevia, S., Cohen, L., Horev, B. and Philosoph-Hadas, S. 1998. Suppression of Botrytis rot in cut rose flowers by postharvest application of methyl jasmonate. Postharvest Biology and Technology, 13: 235-243.

Wang, M., Ling, N., Dong, X., Zhu, Y., Shen, Q. and Guo, S. 2012. Thermographic visualization of leaf response in cucumber plants infected with the soil-borne pathogen *Fusarium oxysporum* f. sp. *Cucumerinum*. Plant Physiology and Biochemistry, 61: 153-161.

[Downloaded from jcp.modares.ac.ir on 2024-10-12]

[DOR: 20.1001.1.22519041.2016.5.4.12.7]

طبقه‌بندی گل‌های رز شاخه بریده آلوده به قارچ *Botrytis cinerea* و تحت تیمار متیل جاسمونات با استفاده از شبکه‌های عصبی تابع شعاعی و باساس ارزیابی تصاویر حرارتی

مهرنوش جعفری[۱]، سعید مینایی[۱]، ناصر صفایی[۲] فرح ترکمنی آذر[۳] و مهدی صادقی[۴]

۱- گروه مهندسی مکانیک بیوسیستم، دانشکده کشاورزی، دانشگاه تربیت مدرس، تهران، ایران.
۲- گروه بیماری شناسی گیاهی، دانشکده کشاورزی، دانشگاه تربیت مدرس، تهران، ایران.
۳- گروه مهندسی برق، دانشکده مهندسی برق و کامپیوتر، دانشگاه شهید بهشتی، تهران، ایران.
۴- گروه علوم باغبانی، دانشکده کشاورزی، دانشگاه تربیت مدرس، تهران، ایران.
* پست الکترونیکی نویسنده مسئول مکاتبه: minaee@modares.ac.ir
دریافت: ۸ آذر ۱۳۹۴؛ پذیرش: ۱ اسفند ۱۳۹۴

چکیده: عوامل محیطی و فیزیولوژیکی متعددی دمای گیاه را تحت تأثیر قرار می‌دهند. هدف پژوهش حاضر، بهره‌گیری از تصویربرداری حرارتی به‌منظور شناسایی ویژگی‌های مناسب در راستای تشخیص زودهنگام آسیب ناشی از قارچ *Botrytis cinerea* در گل‌های رز شاخه بریده که با سطوح مختلفی از متیل جاسمونات (MeJA) تیمار شده بودند، می‌باشد. در این پژوهش، پنج تیمار که شامل سه تیمار با غلظت‌های متفاوت متیل جاسمونات (۰/۱، ۰/۲ و ۰/۳ $\mu l.l^{-1}$)، شاهد ($\mu l.l^{-1}$) و یک تیمار تحت اثر اتانول (۲۰ $\mu l.l^{-1}$ اتانول) بود، درنظر گرفته شد. در طی پنج روز متوالی تصاویر حرارتی تیمارهای تحت تأثیر MeJA و شاهد ثبت و ضبط گردید. ارزیابی روزانه گل‌ها نشان داد که در روز هشتم بعد از مایه‌زنی، شدت بیماری در تیمارهای تحت تأثیر غلظت‌های متفاوت MeJA به میزان قابل‌توجهی کم‌تر از تیمار اتانول و کنترل بود. نتایج نشان داد که حداقل یک روز قبل از بروز هر گونه علائم ظاهری، شاخص‌های بیشینه تفاوت دمایی (MTD) و میانه دمایی می‌توانند به‌منظور شناسایی حضور و رشد پاتوژن مورد استفاده قرار گیرند. به‌منظور شناسایی ویژگی‌های قابل اطمینان در راستای طبقه‌بندی گل‌های سالم و بیمار، آنالیز توزیع فرکانس دمایی مورد مطالعه قرار گرفت. براساس شکل هیستوگرام‌های دمایی، توزیع نرمال و لاپلاس به‌عنوان منطبق‌ترین توزیع‌های احتمال در نظر گرفته شد. توابع چگالی احتمال توزیع نرمال و لاپلاس تخمین زده شد و مؤثرترین ویژگی‌ها انتخاب گردید. یک شبکه عصبی تابع شعاعی با تعداد ۶۰ نرون در لایه مخفی طراحی شد تا گل‌های آسیب دیده را از گل‌های سالم جدا کند. نتایج نشان داد شبکه عصبی طراحی شده قادر است گل‌های بیمار را با نرخ تخمین ۹۶/۴ ٪ از گل‌های سالم تفکیک نماید.

واژگان کلیدی: توزیع لاپلاس، میانه دمایی، توزیع نرمال، هیستوگرام دمایی

[Downloaded from jcp.modares.ac.ir on 2024-10-12]
[DOR: 20.1001.1.22519041.2016.5.4.12.7]